Complementary DNA Cloning and Kinetic Characterization of a Novel Intracellular Serine Proteinase Inhibitor: Mechanism of Action with Trypsin and Factor Xa as Model Proteinases†

Kurt A. Morgenstern,‡ Cindy Sprecher,§ Laurel Holth,§ Donald Foster,§ Francis J. Grant,§ Andrew Ching,§ and Walter Kisiel*,‡

Blood Systems Research Foundation Laboratory, Department of Pathology, University of New Mexico School of Medicine, Albuquerque, New Mexico 87131, and ZymoGenetics, Inc., Seattle, Washington 98105

Received October 7, 1993; Revised Manuscript Received January 5, 1994®

ABSTRACT: The full-length cDNA encoding a novel human intracellular serine proteinase inhibitor has been sequenced and found to encode a 376 amino acid protein ($M_r \approx 42.5$K) that we designate as cytoplasmic antiproteinase. Analysis of the primary structure revealed that the cytoplasmic antiproteinase has the majority of structural motifs conserved among the greater superfamily of serine proteinase inhibitors, or serpins. On the basis of several criteria such as amino acid identity and the absence of a classical N-terminal signal peptide, the cytoplasmic antiproteinase represents a new member of the intracellular serpin family. Further inspection of the cytoplasmic antiproteinase amino acid sequence identified three potential N-glycosylation sites and Arg^{341}-Cys^{342} as the reactive site P_1-P_1' residues, respectively. We have also employed the slow binding kinetic approach to detail the mechanism of bovine trypsin and human factor Xa inhibition by the novel cytoplasmic antiproteinase. Inhibition of trypsin by the cytoplasmic antiproteinase was preceded by a two-step mechanism corresponding to the formation of an initial loose complex, followed by an isomerization step to a more stable, tight complex. The binding of the cytoplasmic antiproteinase to trypsin occurred with a second-order association rate constant of 2.8×10^6 M^{-1} s^{-1} and an overall equilibrium constant of 22.5 pM, demonstrating that the factor is a potent inhibitor of this proteinase. Under the appropriate conditions, the tight complex between trypsin and the cytoplasmic inhibitor was reversible, indicated by an exponential regeneration of proteinase amidolytic activity from the preformed complex. Therefore, the tight complex appears to be stabilized predominantly by reversible bonds that form between trypsin and the cytoplasmic inhibitor. In contrast to the inhibition of trypsin, the inhibition of factor Xa amidolytic activity by the cytoplasmic antiproteinase followed a single-step binding mechanism. The apparent first-order rate constant for factor Xa inhibition was found to increase as a linear function of the inhibitor concentration range studied. Formation of the inhibitory complex between factor Xa and the cytoplasmic antiproteinase occurred with a second-order association rate constant of approximately 1.3×10^5 M^{-1} s^{-1} and a equilibrium constant of 3.7 nM. These findings suggests that the cytoplasmic inhibitor may initially encounter significant energy barriers for proper alignment with the substrate binding cleft of factor Xa. However, once aligned, the reaction proceeds rapidly to a tight factor Xa·inhibitor complex that dissociates at a slow rate.

Serine proteinases with trypsin-like specificity play an essential role in the activation of many extracellular physiological processes including blood coagulation (Davie et al., 1991), complement activation (Reid et al., 1981), fibrinolysis (Astrup et al., 1978), and cell growth and migration (Saksela et al., 1988), to name a few. The proteinase-mediated activation step in these processes involves the irreversible hydrolysis of specific peptide bonds in key substrates (Neurath, 1984). The specificity of substrate activation is dictated largely by a highly developed complementary interaction between the proteinase active site region and the cleavage site of the physiological substrate(s). The catalytic activities of extracellular serine proteinases are tightly regulated by a superfamily of proteinase inhibitors that typically range between 50 and 110 kDa in molecular mass (Carrell & Boswell, 1986; Carrell et al., 1987). This superfamily of serine proteinase inhibitors, or serpins, includes a number of homologous proteins that resemble α_1-proteinase inhibitor in overall structure and includes antithrombin III, α_2-antiplasmin, plasminogen activator inhibitors 1 and 2, and α_1-antichymotrypsin (Carrell et al., 1987; Huber & Carrell, 1989). Serpin molecules are composed of three β-sheets surrounded by eight α-helices, and their proteinase-inhibitory specificity is defined by the P_1-P_1' residues located within the reactive-site loop (Huber & Carrell, 1989; Lodermann et al., 1984; Schechter & Berger, 1967). Recent kinetic studies with α_2-antiplasmin (Longstaff & Gaffney, 1991), antithrombin III (Olson & Shore, 1982), and α_1-proteinase inhibitor (Bruch & Bieth, 1989; Faller et al., 1993) have demonstrated a two-step mechanism for the inhibition of their cognate proteinase targets. In general, this mechanism involved the formation of an initial loose complex that further isomerizes to a tight complex, resulting in the pseudoreversible arrest of proteolysis. The serpin reactive-site domain exhibits a high degree of divergence between serpin members and exists as a stressed loop with a canonical conformation that confers optimal binding to the substrate binding cleft of the cognate proteinase (Bode & Huber, 1992). This initial interaction between proteinase and inhibitor may

† This work was supported by a grant from the Blood Systems Research Foundation.

* To whom correspondence should be addressed.

‡ University of New Mexico.

§ ZymoGenetics, Inc.

® Abstract published in *Advance ACS Abstracts*, February 15, 1994.

0006-2960/94/0433-3432$04.50/0

represent what has been defined kinetically as the loose complex. Isomerization to the tight complex results in the formation of a reversible tetrahedral intermediate between the γ-OH group of the proteinase active site serine residue and the carbonyl carbon of the serpin P_1-P_1' scissile peptide bond (Matheson et al., 1991). The stability of the tetrahedral intermediate is likely to be a property unique to each individual serpin and the corresponding interactions with the bound proteinase. Formation of a stable complex between the serpin and the active site of the serine proteinase involves relaxation of the strain imposed on the native reactive-site loop (Carrell & Boswell, 1986). This occurs by the partial insertion of the proteinase-bound reactive-site loop into the central A-β-sheet of the serpin (Björk et al., 1992, 1993; Skriver et al., 1991). The conformational change induced in the serpin appears to be essential for the exposure of a receptor recognition domain that mediates cell surface binding of the proteinase–serpin complex and clearance (Joslin et al., 1993; Mast et al., 1991).

In addition to the serpins that regulate proteinase activity, several members of this superfamily lack a proteinase-inhibitory capability and have other physiological roles. These latter serpins were originally identified by data base searching and include thyroxine binding globulin (Flink et al., 1986), angiotensinogen (Doolittle, 1983), and ovalbumin (Hunt & Dayhoff, 1980). Ovalbumin represents the parent prototype of a unique family, within the serpin superfamily, that lack a typical cleavable signal sequence, but have been found to reside either intracellularly, extracellularly, or both (Remold-O'Donnell, 1993). The serpins previously classified as members of the ovalbumin branch are plasminogen activator inhibitor 2 (PAI-2)[1] (Ye et al., 1989), an elastase inhibitor isolated from monocyte-like cells (EI) (Dubin et al., 1992; Remold-O'Donnell et al., 1992), and a squamous cell carcinoma antigen (SCCA) (Suminami et al., 1991). Recently, we have isolated a 38-kDa serine proteinase inhibitor from the cytosolic fraction of a kidney epithelial cell line (Morgenstern et al., 1993). The cytosolic factor inhibited the amidolytic activities of trypsin, thrombin, and factor Xa with apparent association rate constants of 8×10^6 M^{-1} s^{-1}, 5×10^5 M^{-1} s^{-1}, and 1.5×10^5 M^{-1} s^{-1}, respectively (Morgenstern et al., 1993). Therefore, we have designated the 38-kDa inhibitor as cytoplasmic antiproteinase, or CAP, to reflect its cellular localization and biological activity. Partial sequence analysis revealed that CAP contained structural motifs conserved among the greater serpin superfamily (Morgenstern et al., 1993) and was identical to a novel thrombin inhibitor isolated in a functionally inactive form from human placenta (Coughlin et al., 1993). In all likelihood, CAP is identical to a cytoplasmic factor originally identified by Kirshner and co-workers (Kirshner et al., 1980) and subsequently found to form an SDS-stable complex with trypsin, urokinase, plasmin, and thrombin in a heparin-independent manner (Eaton & Baker, 1983). In the present work, we report the full-length complementary DNA sequence that encodes human CAP and demonstrate that this novel inhibitor displays multiple structural features characteristic of the ovalbumin family of cytoplasmic serpins. In addition, we have performed a detailed kinetic analysis of CAP and have deduced its mechanism of inhibition using trypsin and factor Xa as model target proteinases.

[1] Abbreviations: PAI-2, plasminogen activator inhibitor 2; EI, elastase inhibitor; SCCA, squamous cell carcinoma antigen; CAP, cytoplasmic antiproteinase; TPCK–trypsin, *N*-tosyl-L-phenylalanine chloromethyl ketone-treated trypsin; S-2288, H-D-Ile-Pro-Arg-*p*-nitroanilide; S-2222, benzyl-Ile-Glu-Gly-Arg-*p*-nitroanilide; BSA, bovine serum albumin; PMSF, phenylmethanesulfonyl fluoride; β-ME, 2-mercaptoethanol; EDTA, (ethylenedinitrilo)tetraacetic acid; Hepes, 4-(2-hydroxyethyl)-1-piperazineethanesulfonic acid; PCR, polymerase chain reaction; kb, kilobases; SDS, sodium dodecyl sulfate.

MATERIALS AND METHODS

A human cDNA placental library and tissue-specific poly-$(A)^+$ mRNA samples for Northern analysis were purchased from ClonTech (Palo Alto, CA). Bovine TPCK–trypsin was purchased from Worthington (Freehold, NJ) and reconstituted in 1 mM HCl (pH 3.0), and aliquots (2.0 mg/mL) were stored at −80 °C. The substrates H-D-Ile-Pro-Arg-*p*-nitroanilide (S-2288) and benzyl-Ile-Glu-Gly-Arg-*p*-nitroanilide (S-2222) were obtained from Kabi/Pharmacia (Franklin, OH) and reconstituted in double-distilled water, and 10 mM aliquots were stored at −20 °C. Hepes (free acid), sodium chloride, benzamidine, *p*-nitrophenyl-*p*-guanidinobenzoate (NPGB), leupeptin, and bovine serum albumin (fatty acid-free) were purchased from Sigma Chemical Co (St. Louis, MO). BSA was further purified by Blue-Sepharose CL-6B affinity chromatography and found to be devoid of any proteinase-inhibitory activity (Travis et al., 1976). Heparin–Sepharose was prepared by coupling heparin to CNBr-activated Sepharose 4B (Pharmacia LKB Biotechnology Inc., Alameda, CA) essentially as described (Kisiel & Davie, 1975). Human factor Xa and antithrombin III were purified by methods described previously (Kondo & Kisiel, 1987; Mahoney et al., 1980). Microtitration plates (96 well) were purchased from Dynatech Laboratories (Chantilly, VA).

cDNA Isolation and Sequencing. The peptides DIHQGFQ and GKIAEL were obtained by manually sequencing cyanogen bromide cleavage products of CAP previously purified to homogeneity from a monkey kidney epithelial cell line (Morgenstern et al., 1993). These peptides were used to design degenerate oligonucleotides used for PCR amplification of CAP cDNA from a human placental library. The 209 bp sequence between the two PCR primers was labeled with ^{32}P-nucleotides by random priming and used as a probe to screen a human placental cDNA λGT11 library, constructed and kindly provided by Dr. Fred Hagen (ZymoGenetics, Inc.). Nylon membranes containing a total of 8×10^5 plaques were screened by hybridization at 65 °C in 5× SSPE/5× Denhardt's/0.5% SDS/100 μg/mL salmon sperm DNA. Filters were washed at 65 °C in 0.2× SSC/0.1% SDS. Positive plaques were purified and the three largest cDNA inserts were amplified using PCR and sequenced by the dideoxy chain-termination method (Sanger et al., 1977).

Northern Analysis. Poly$(A)^+$ RNAs from various human tissues (5 μg/lane) were denatured, electrophoresed, transferred to a nylon membrane, and probed with a ^{32}P-end-labeled CAP oligonucleotide (5′-CTGCGTGCCAGTCTTGTTCAC-TTCGGTGAGAAGAGA-3′) essentially as described (Maniatis et al., 1989). Hybridization was performed at 55 °C in 5× SSPE/2× Denhardt's/0.5% SDS/100 μg/mL salmon sperm DNA. The blots was washed at 55 °C in 2× SSC/0.1% SDS and exposed to autoradiography.

Isolation of CAP from Human Placenta. The cytoplasmic antiproteinase was purified to homogeneity from human placenta by a modification of the procedure previously described (Morgenstern et al., 1993). Whole placenta (approximately 650 g/L) was homogenized in 20 mM Hepes (pH 7.5)/2 mM β-ME/50 mM benzamidine/0.2 mM PMSF/2 mM EDTA/2 μg/mL leupeptin. The homogenate was centrifuged (4200*g*/4 °C/1 h) using a Beckman Model J-6ME centrifuge equipped with a JS-4.2 rotor. The clarified supernatant was then stored at −80 °C. Prior to fractionation

by column chromatography, approximately 100 mL (20 mg/mL) of placental homogenate was thawed at 25 °C and centrifuged (100000*g*/4 °C/30 min) in a Beckman Model L5-75 ultracentrifuge equipped with a type 65 rotor. The resulting supernatants were pooled and applied at a flow rate of 0.5 mL/min to a Pharmacia K25/70 column packed with 325 mL of heparin–Sepharose. Approximately 150 mg of the heparin–Sepharose unadsorbed fraction was then applied at a flow rate of 0.5 mL/min to a Pharmacia HR 10/10 column packed with 8.0 mL of Q-Sepharose fast-flow resin (Pharmacia/LKB). The ion-exchange column was connected to a Pharmacia FPLC system and washed at 4.0 mL/min with 30 mL of 20 mM Hepes (7.5)/2 mM β-ME followed by a linear salt gradient ranging from 0 to 0.3 M NaCl (10 mM NaCl/min) in the same buffer. Fractions containing CAP activity were pooled (~35 mL; 0.4 mg/mL) and applied to a Pharmacia HR 5/5 column packed with 1.0 mL of anhydrotrypsin–Affi-Gel 10. The anhydrotrypsin–Affi-Gel 10 affinity column was washed and the cytoplasmic antiproteinase eluted at pH 4.0 into 0.01% BSA (Morgenstern et al., 1993). The eluate fractions obtained from anhydrotrypsin affinity chromatography were pooled and dialyzed against 2 L of 20 mM Hepes (7.5)/0.15 M NaCl overnight at 4 °C, aliquoted, and stored at −80 °C. This procedure yielded approximately 15–20 μg of functionally active CAP/g of placental protein.

General Kinetic Methods. The concentration of catalytically active TPCK–trypsin was determined by titration with *p*-NPGB as previously described (Chase & Shaw, 1969). Active site titrated TPCK–trypsin was then used to measure the reactive concentration of purified CAP. TPCK–trypsin (7.8 nM) was mixed with increasing aliquots of CAP in a total volume of 0.1 mL of 20 mM Hepes (7.5)/0.15 M NaCl/0.01% BSA. The reactants were incubated for 30 min at 37 °C in individual wells of a microtitration plate previously blocked with buffer containing 0.01% BSA. Residual TPCK–trypsin amidolytic activity was measured upon the addition of 0.1 mL of 20 mM Hepes (7.5)/0.15 M NaCl/0.01% BSA/1.0 mM S-2288 by monitoring the enzymatic production of *p*-nitroaniline for 5 min at 405 nm using a UV_{max} kinetic microtitration plate autoreader (Molecular Devices, Inc.). The enzymatic rate of substrate hydrolysis was then plotted as a function of the CAP volume added to each reaction well. Linear regression to the *x*-axis enabled the precise concentration of reactive CAP to be calculated. The catalytically active concentration of factor Xa was determined by a similar approach using titrated antithrombin III in the presence of 6.7 units/mL heparin as described previously (Morgenstern et al., 1993).

Catalytic constants for TPCK–trypsin were measured in 20 mM Hepes (7.5)/0.15 M NaCl/0.01% BSA at 25 °C with S-2288 as the substrate. The K_m and k_{cat} under these conditions were 0.03 mM and 118 s^{-1}, respectively. Factor Xa was assayed using the same conditions employed for TPCK–trypsin except 0.5% glycerol was included in the buffer and S-2222 was the substrate. The corresponding catalytic constants were K_m = 0.25 mM and k_{cat} = 45 s^{-1}.

Slow-Binding Inhibition Kinetics. Inhibitor progress curves were obtained by incubating the reactants at 25 °C in 0.5 mL of the same buffer used to determine the catalytic constants. The proteinase (0.1 mL) was added to polystyrene cuvettes previously blocked with 20 mM Hepes (7.5)/0.15 M NaCl/0.01% BSA. The cuvettes were placed in a Beckman DU-65 spectrophotometer equipped with a six-cell cuvette holder so that multiple reactions could be monitored simultaneously at 405 nm. A total of six reactions were initiated within 30 s by adding a solution (0.4 mL) containing the chromogenic substrate and the appropriate concentration of inhibitor to the cuvettes. For experiments with TPCK–trypsin, the final concentrations of reactants were 0.25 nM proteinase, 0.5 mM S-2288, and 0, 2.5, 5.0, 7.5, 10.0, and 12.5 nM CAP. For experiments with factor Xa, the final concentrations of reactants were 0.3 nM proteinase, 0.75 mM S-2222, and 0, 10, 15, 20, 25, and 30 nM CAP. Spontaneous substrate hydrolysis was determined in separate control experiments, and in some cases a constant amount of *p*-nitroaniline was read to account for instrument drift. The amount of substrate hydrolyzed by either proteinase during the course of an experiment was less than 10% of the total substrate present at zero time unless indicated.

The reactions were allowed to proceed until steady-state velocity was attained, and the data were then fitted to the integrated rate equation for slow-binding inhibition (Morrison & Walsh, 1988):

$$A = v_s t + (v_0 - v_s)(1 - e^{-k't})/k' + A_0 \qquad (1)$$

by nonlinear regression analysis using Enzfitter software (Leatherbarrow, 1987). Regression analysis provided values for the initial velocity (v_0), the steady-state velocity (v_s), the initial absorbance at zero time (A_0), and the apparent first-order rate constant (k') for the establishment of steady-state equilibrium between proteinase–inhibitor complexes. The variables v_0, v_s, and k' were then used in various previously described graphical transformations (Cha, 1975; Longstaff & Gaffney, 1991; Morrison, 1982; Morrison & Walsh, 1988; Shapiro & Riordan, 1984) to obtain the inhibition constants and rate constants for the interaction of CAP with the target proteinase.

Dissociation of Preformed Complexes. The experimental approach used to dissociate the TPCK–trypsin·CAP complex was adopted from the procedure previously employed to study the stability of the chymotrypsin·α_2-antiplasmin complex (Longstaff & Gaffney, 1991). A complex of TPCK–trypsin and CAP was made by incubating 0.14 μM inhibitor (10 μL) with 0.18 μM (2 μL) proteinase for 1 h on ice. The complex was then diluted approximately 10^3-fold into a 1.5 mL of buffer containing 2.0 mM S-2288 at 25 °C. The regeneration of TPCK–trypsin amidolytic activity was monitored at 2-min intervals for 5 h. The k' for this reaction was obtained by fitting the data to eq 1 using Enzfitter software (Leatherbarrow, 1987). The first-order rate constant, k_{-2}, for the reactivation of the loose complex was determined from the following relationship for k' (see Results):

$$k' = k_{-2}(1 + [I]/K_{i(app)}')/(1 + [I]/K_{i(app)}) \qquad (2)$$

where $K_{i(app)}' = K_i'(1 + [S]/K_m)$ and $K_{i(app)} = K_i(1 + [S]/K_m)$ (Morrison & Walsh, 1988).

RESULTS

The full-length cDNA that encodes CAP was sequenced and estimated to be 1.46 kb in length (Figure 1). Five positive clones with the CAP cDNA insert were sequenced and found to each contain a unique nucleotide sequence upstream from adenine 177, while the nucleotide sequences downstream of this position were found to be invariant in all cases (data not shown). The CAP cDNA sequences had a large open reading frame beginning with the ATG codon at nucleotide 186. This codon is likely to represent the methionine at the translational start site since the flanking nucleotides ATCATGG represent

```
GAATTCGGGTCTCGAGCAGGAAGTACCAAGGGAGGATGGAGATGGTAATAATCAGGGTTGGGTGGAGAA   69

TATCTGAGGAAACTGCACTTGATTTGGGCCTTGAAGAGTAATTGACTGGATTTAGATTTATCTAGAAAG  138

GTCGTTCCCAGCAGAAGCAACAAGAACAACAAGCTTGGAGGTCTGCCATCATGGATGTTCTCGCAGAAG  207
                                        ^          M  D  V  L  A  E  A
                                                   1
CAAATGGCACCTTTGCCTTAAACCTTTTGAAAACGCTGGGTAAAGACAACTCGAAGAATGTGTTTTTCT  276
  N  G  T  F  A  L  N  L  L  K  T  L  G  K  D  N  S  K  N  V  F  F  S
     10                            20                            30
CACCCATGAGCATGTCCTGTGCCCTGGCCATGGTCTACATGGGGGCAAAGGGAAACACCGCTGCACAGA  345
  P  M  S  M  S  C  A  L  A  M  V  Y  M  G  A  K  G  N  T  A  A  Q  M
                           40                            50
TGGCCCAGATACTTTCTTTCAATAAAAGTGGCGGTGGTGGAGACATCCACCAGGGCTTCCAGTCTCTTC  414
  A  Q  I  L  S  F  N  K  S  G  G  G  G  D  I  H  Q  G  F  Q  S  L  L
                    60                            70
TCACCGAAGTGAACAAGACTGGCACGCAGTACTTGCTTAGGGTGGCCAACAGGCTCTTTGGGGAAAAGT  483
  T  E  V  N  K  T  G  T  Q  Y  L  L  R  V  A  N  R  L  F  G  E  K  S
        80                            90
CTTGTGATTTCCTCTCATCTTTTAGAGATTCCTGCCAAAAATTCTACCAAGCAGAGATGGAGGAGCTTG  552
  C  D  F  L  S  S  F  R  D  S  C  Q  K  F  Y  Q  A  E  M  E  E  L  D
100                           110                           120
ACTTTATCAGCGCCGTAGAGAAGTCCAGAAAACACATAAACACCTGGGTAGCTGAAAAGACAGAAGGTA  621
  F  I  S  A  V  E  K  S  R  K  H  I  N  T  W  V  A  E  K  T  E  G  K
                    130                           140
AAATTGCGGAGTTGCTCTCTCCGGGCTCAGTGGATCCATTGACAAGGCTGGTTCTGGTGAATGCTGTCT  690
  I  A  E  L  L  S  P  G  S  V  D  P  L  T  R  L  V  L  V  N  A  V  Y
           150                           160
ATTTCAGAGGAAACTGGGATGAACAGTTTGACAAGGAGAACACCGAGGAGAGACTGTTTAAAGTCAGCA  759
  F  R  G  N  W  D  E  Q  F  D  K  E  N  T  E  E  R  L  F  K  V  S  K
 170                           180                           190
AGAATGAGGAGAAACCTGTGCAAATGATGTTTAAGCAATCTACTTTTAAGAAGACCTATATAGGAGAAA  828
  N  E  E  K  P  V  Q  M  M  F  K  Q  S  T  F  K  K  T  Y  I  G  E  I
                         200                           210
TATTTACCCAAATCTTGGTGCTTCCATATGTTGGCAAGGAACTGAATATGATCATCATGCTTCCGGACG  897
  F  T  Q  I  L  V  L  P  Y  V  G  K  E  L  N  M  I  I  M  L  P  D  E
                  220                           230
AGACCACTGACTTGAGAACGGTGGAGAAAGAACTCACTTACGAGAAGTTCGTAGAATGGACGAGGCTGG  966
  T  T  D  L  R  T  V  E  K  E  L  T  Y  E  K  F  V  E  W  T  R  L  D
     240                           250                           260
ACATGATGGATGAAGAGGAGGTGGAAGTGTCCCTCCCGCGGTTTAAACTAGAGGAAAGCTACGACATGG 1035
  M  M  D  E  E  E  V  E  V  S  L  P  R  F  K  L  E  E  S  Y  D  M  E
                           270                           280
AGAGTGTCCTGCGCAACCTGGGCATGACTGATGCCTTCGAGCTGGGCAAGGCAGACTTCTCTGGAATGT 1104
  S  V  L  R  N  L  G  M  T  D  A  F  E  L  G  K  A  D  F  S  G  M  S
                    290                           300
CCCAGACAGACCTGTCTCTGTCCAAGGTCGTGCACAAGTCTTTTGTGGAGGTCAATGAGGAAGGCACGG 1173
  Q  T  D  L  S  L  S  K  V  V  H  K  S  F  V  E  V  N  E  E  G  T  E
        310                           320
AGGCTGCAGCCGCCACAGCTGCCATCATGATGATGCGGTGTGCCAGATTCGTCCCCCGCTTCTGCGCCG 1242
  A  A  A  A  T  A  A  I  M  M  M  R  C  A  R  F  V  P  R  F  C  A  D
330                           340    ▲                      350
ACCACCCCTTCCTTTTCTTCATCCAGCACAGCAAGACCAACGGGATTCTCTTCTGCGGCCGCTTTTCCT 1311
  H  P  F  L  F  F  I  Q  H  S  K  T  N  G  I  L  F  C  G  R  F  S  S
                    360                           370
CTCCGTGAGGACAGGGCAGTCTTGGTGTGCAGCCCCTCTCCTCTCTGTCCCCTGACACTCCACAGTGTG 1380
  P  ***
376
CCTGCAACCCAAGTGGCCTTATCCGTGCAGTGGTGGCAGTTCAGAAATAAAGGGCCCATTTGTGGGATG 1449

CCGCATTAAAAAAAAA 1465
```

FIGURE 1: The complete complementary DNA sequence and the corresponding amino acid sequence of human CAP. The 5′-untranslated region upstream from the caret (∧) was found to be divergent among five different cDNA clones that were isolated and sequenced. The authentic termination codon is designated by triple asterisks, and the polyadenylation signal sequence is underlined. The N-glycosylation consensus sites are loctated at Asn-8, Asn-60, and Asn-80. The reactive-site P_1-P_1' residues of CAP are indicated by boldface type, and the peptide bond cleavage site is designated by an arrow.

part of an optimal initiation signal for association of the activated 40S ribosomal subunit (Kozak, 1986). The 5′-region in the CAP cDNA sequence shown in Figure 1 has several additional inframe putative ATG codons starting with nucleotides 36 and 42. However, these alternative translational start sites are flanked by a less than optimal initiation nucleotide sequence (Kozak, 1986), and the translation process would be aborted by the termination codons TAA and TAG beginning at nucleotides 108 and 132, respectively. The authentic termination codon was identified near the 3′-end of the transcript approximately 109 residues upstream from the nascent mRNA cleavage and polyadenylation signal, AATAAA (Moore & Sharp, 1985) (Figure 1). Northern blot analysis revealed a single hybridizing mRNA species in human placenta of approximately 1.4 kb (data not shown), indicating that the cDNA sequence reported is complete. In addition to placenta, the 1.4-kb transcript was also detected in human cardiac muscle, lung, liver, skeletal muscle, kidney, and pancreas. In contrast, no mRNA for CAP was detected in human brain tissue. Of the positive tissues, skeletal muscle appeared to express the highest levels of the 1.4-kb mRNA, a finding that correlates with the original observation that cultured myotubes express high levels of CAP activity relative to other cell lines (Eaton & Baker, 1983).

The identified open reading frame in the 1.4-kb cDNA encoded a 376 amino acid protein (M_r = 42 594) with a composition consisting of Gly_{22}, Ala_{25}, Val_{25}, Leu_{36}, Ile_{13}, Ser_{28}, Cys_6, Thr_{23}, Met_{19}, Phe_{28}, Tyr_8, Trp_3, Pro_{10}, His_5, Lys_{27}, Arg_{15}, Asp_{18}, Glu_{35}, Asn_{17}, and Gln_{13}. The primary structure of CAP was found to contain 44 of the 51 residues previously designated as essential for the overall tertiary structure of α_1-proteinase inhibitor and the greater serpin superfamily (Huber & Carrell, 1989; Lodermann et al., 1984). This value of conserved residues in the cytoplasmic inhibitor includes an Ile to Val switch in CAP at residue 188 of α_1-proteinase inhibitor. Importantly, CAP showed significant identity with the serpin superfamily in regions corresponding to helix B (residues 30–44) and strands B4 (residues 354–363), B5 (residues 365–376), and A3 (residues 160–173). These structural elements form the apolar core and the spine of the inhibitor molecule (Huber & Carrell, 1989). Therefore, CAP appears to contain the majority of structural elements that conform to the highly ordered tertiary structure of other known serpins.

The cytoplasmic antiproteinase showed greatest identity with PAI-2 (~49%), EI (~51%), and SCCA (~47%), suggesting that CAP represents a new member of the ovalbumin family of intracellular serpins. The ovalbumin family of serpins have multiple structural characteristics that distinguish them from other proteins in the serpin superfamily (Remold-O'Donnell, 1993). The cytoplasmic antiproteinase exhibited all of these features which can be summarized as follows: (1) CAP lacks an N-terminal extension, and the open reading frame begins at amino acid 23 of α_1-proteinase inhibitor; (2) CAP lacks a C-terminal extension terminating at Pro-376, the equivalent of Pro-391 of α_1-proteinase inhibitor; (3) CAP has a Ser at position 375 in place of a highly conserved Asn found among all serpins distantly related to the ovalbumin family. Another prominent characteristic that further links CAP to the ovalbumin family of serpins is the absence of an N-terminal cleavable hydrophobic signal sequence (Figure 1). Inspection of the N-terminal region of CAP revealed several hydrophilic residues such as asparagine, aspartic acid, glutamic acid, and lysine that would be incompatible with a membrane insertion domain. CAP also has three potential N-glycosylation consensus sites (N-X-T/S) located at Asn-8, Asn-60, and Asn-80 (Figure 1). The former two N-glycosylation consensus sequences at residues 8 and 60 are unique to CAP, while the latter site at residue 80 is shared among PAI-2 and SCCA.

Alignment of the deduced primary structure of CAP with the amino acid sequences of PAI-2, SCCA, and EI identified the CAP reactive center P_1-P_1' residues as Arg-341 and Cys-342, respectively (Figure 1). Interestingly, Arg-341 was flanked by a series of Met residues in the P_2–P_4 positions and several Arg residues in the P_3' and P_7' positions, a region thought to participate in proteinase docking (Huber & Carrell, 1989). These molecular features of the CAP reactive center region are uncommon among members of the mammalian serpin superfamily. Therefore, we performed a detailed kinetic analysis to characterize the mechanism by which CAP inhibits several model extracellular serine proteinases including bovine TPCK–trypsin and human factor Xa.

Preliminary studies suggested that CAP obeyed slow-binding inhibition kinetics. Slow-binding behavior was indicated by the observation that CAP-mediated inhibition of proteinase amidolytic activity approached steady-state equilibrium on a time scale of minutes under the experimental conditions employed and the data could be successfully fitted

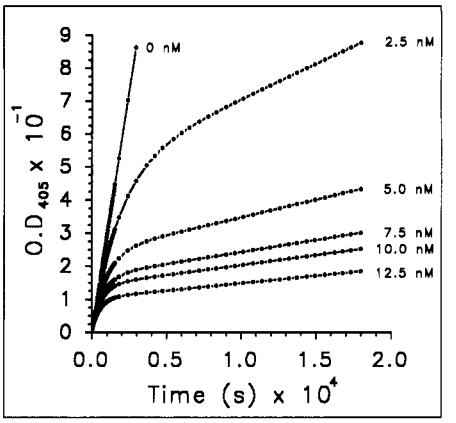

FIGURE 2: Slow-binding kinetics for the inhibition of TPCK–trypsin by CAP. TPCK–trypsin (0.25 nM) was reacted with 0, 2.5, 5.0, 7.5, 10.0, and 12.5 nM CAP in 20 mM Hepes (7.5)/0.15 M NaCl/0.01% BSA/0.5 mM S-2288. The reactions were monitored continuously for 5 h at 405 nm, and the data were fitted to eq 1 to generate values for the variables v_0, v_s, and k' (Materials and Methods). The depletion of substrate was approximately 16% in the reaction with 2.5 nM CAP. In all cases, the upper limit of product generation used to determine steady-state rates was within the linear range of the uninhibited TPCK–trypsin control.

to the slow-binding equation (eq 1) (Morrison & Walsh, 1988). There are three mechanisms that describe the observed slow onset of inhibition (Cha, 1975):

mechanism A:

$$P \underset{k_{-1}}{\overset{k_1[I]}{\rightleftharpoons}} PI$$

mechanism B:

$$P \underset{k_{-1}}{\overset{k_1[I]}{\rightleftharpoons}} PI \underset{k_{-2}}{\overset{k_2\,(slow)}{\rightleftharpoons}} PI'$$

mechanism C:

$$P \underset{k_{-1}}{\overset{k_1\,(slow)}{\rightleftharpoons}} P' \underset{k_2}{\overset{k_2[I]}{\rightleftharpoons}} P'I$$

In mechanism (or scheme) A, proteinase (P) binds to the inhibitor (I) in a slow step to form a PI complex. In mechanism B, a loose PI complex forms rapidly followed by a slow isomerization to a tight PI′ complex. In mechanism C, the proteinase undergoes a slow isomerization to P′ and then rapidly forms a tight P′I complex. These mechanisms can be distinguished by applying the slow-binding kinetic approach previously described (Morrison & Walsh, 1988).

To simplify data interpretation, kinetic characterization of CAP was performed under pseudo-first-order conditions in which the lowest concentration of CAP was at least in 10-fold excess of the proteinase. Figure 2 shows a family of inhibition progress curves that are representative of the reaction between CAP and TPCK–trypsin as a function of CAP concentration. As the concentration of CAP was increased, the initial burst phase of each progress curve was shorter and the curves turned over faster, representing the approach toward steady-state equilibrium. Data from each inhibition progress curve were fitted to eq 1, and values for the variables v_0, v_s, and k' were generated. The initial velocity, v_0, was found to be inversely related to the concentration of CAP, suggesting that the inhibition of TPCK–trypsin by CAP occurs through a two-step mechanism described by scheme B (Morrison & Walsh,

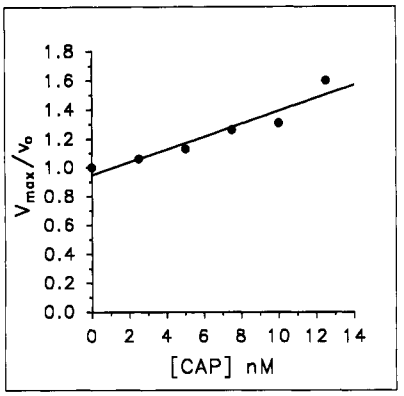

FIGURE 3: Determination of the dissociation constant for the TPCK–trypsin·CAP loose complex. A representative plot of V_{max}/v_0 versus [CAP] for the determination of K_i. The values for v_0 were obtained as described in the legend to Figure 2. From the slope of the line, K_i was calculated using the relationship: $V_{max}/v_0 = K_m[I]/[S]K_i + (1 + K_m/[S])$ (Longstaff & Gaffney, 1991; Morrison & Walsh, 1988).

1988). The initial velocity data did not conform to a single-step mechanism described by scheme A since v_0 is predicted to be independent of the inhibitor concentration (Morrison & Walsh, 1988). The apparent first-order rate constant, k', was found to increase with an increase in CAP concentration. These data are in agreement with schemes A and B, but eliminate scheme C. In the mechanism described by scheme C, k' is predicted to decrease with inhibitor concentration (Shapiro & Riordan, 1984). Therefore, on the basis of these results, and additional evidence reported herein, the data obtained for the inhibition of TPCK–trypsin by CAP were treated in various ways to determine the reaction constants associated with the two-step mechanism described by scheme B.

The dissociation constant, K_i, for the formation of the initial loose complex between TPCK–trypsin and CAP was determined from plots of V_{max}/v_0 versus CAP concentration, which were linear in all cases (Figure 3). The K_i was estimated from the slope of the line to be 2.0 nM (±0.7, SD, n = 4). The overall second-order association rate constant, k_{assoc}, was approximated from the slope of the line generated from a plot of $\log_{10}([P]_\infty - [P]_t)$ versus time, where $[P]_\infty = v_0/k'$ and $[P]_t$ is the optical density measured at various times between 0 and 20 min for an individual inhibition progress curve (data not shown) (Tian & Tsou, 1982). The negative slope of such a plot is $-0.43[I](k_{assoc}/1 + [S]/K_m)$, from which k_{assoc} was estimated to be 2.8×10^6 M^{-1} s^{-1} ($\pm 0.17 \times 10^6$, SD, n = 5). In these calculations, the value of $[P]_\infty$ was found to be consistently lower than the maximal value of optical density experimentally measured for the progress curves obtained at each concentration of CAP. This apparent discrepancy is probably inherent in the approach used since the method derived by Tain and Tsou (1982) does not take into consideration the establishment of steady-state equilibrium between TPCK–trypsin·CAP complexes. Accordingly, k_{assoc} was calculated using the data collected at the early time points up to the initial onset of equilibrium.

The overall inhibition constant, K_i', for the binding of CAP to TPCK–trypsin was determined from plots of V_{max}/v_s versus CAP concentration (data not shown). The K_i' was estimated from the slope of the line to be 23 pM (±2.4, SD, n = 4). Similarly, K_i' was estimated to be 22 pM (±3.0, SD, n = 4) from plots of $(v_0 - v_s)/v_s$ versus CAP concentration (data not shown).

To determine the individual first-order rate constants for the formation and dissociation of the TPCK–trypsin·CAP tight complex, the v_0/v_s ratios were plotted against the values of k' obtained for each CAP concentration studied (Figure 4). These plots passed through the origin and from the slope of the line k_{-2} was determined to be 5.0×10^{-5} s^{-1} ($\pm 0.5 \times 10^{-5}$, SD, n = 4). From the relationship $T_{1/2} = 0.693/k_{-2}$, a half-life of 3.7 h was estimated for the reverse isomerization step to the loose complex. Given the relatively fast rate for the reverse isomerization step, we attempted to demonstrate directly the reversibility of TPCK–trypsin inhibition by CAP. This was accomplished by diluting the preformed TPCK–trypsin·CAP complex into a concentrated solution of substrate such that the complex was approximately 7-fold less than $K_i'_{(app)}$ and the $[S]/K_m$ ratio was 67. Figure 5 shows that TPCK–trypsin amidolytic activity was slowly recovered from the inhibitory complex (curve 1), indicated by the gradual nonlinear increase in substrate hydrolysis relative to the uninhibited TPCK–trypsin control (curve 2). An accurate value of k' was obtained from the concave-up curve by fitting the data to eq 1 (Morrison & Walsh, 1988). In this case, k' represents the rate for reestablishment of steady-state equilibrium between TPCK–trypsin and TPCK–trypsin·CAP complexes after dilution. Equation 2 was then used to determine k_{-2} from k'. Under conditions of high dilution and a high $[S]/K_m$ ratio, the term $(1 + [I]/K_i'_{(app)})/(1 + [I]/K_{i(app)})$ in eq 2 tends toward unity

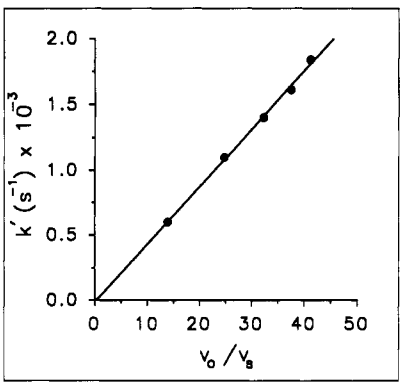

FIGURE 4: Determination of k_{-2} for the dissociation of the TPCK–trypsin·CAP tight complex. Values for v_0, v_s, and k' were obtained as described in the legend to Figure 2. The first-order rate constant, k_{-2}, was determined directly from the slope of the line according to the relationship $k' = k_{-2}(v_0/v_s)$ (Morrison, 1982).

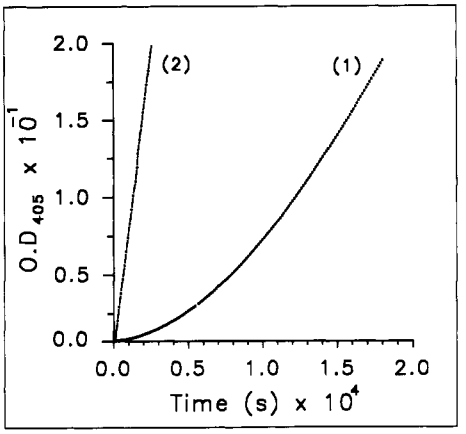

FIGURE 5: Dissociation of the TPCK–trypsin·CAP complex. Curve 1: The preformed TPCK–trypsin·CAP complex (Materials and Methods) was diluted 860-fold into 20 mM Hepes (7.5)/0.15 M NaCl/0.01% BSA containing 2.0 mM S-2288 to give a total enzyme concentration of 0.25 nM. The regeneration of TPCK–trypsin amidolytic activity was monitored continuously as a function of time against a substrate blank. The values for v_0, v_s, and k' were generated by fitting the dissociation data to eq 1 (Materials and Methods). k_{-2} was determined by using eq 2 under conditions where $k' \approx k_{-2}$ (see Results). Curve 2: The parallel uninhibited TPCK–trypsin control.

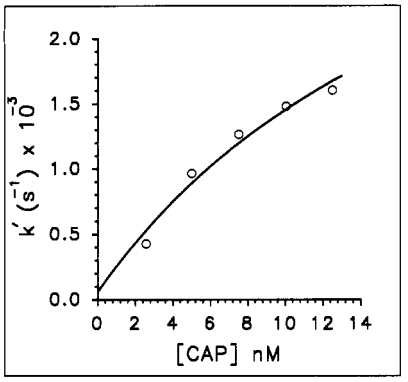

FIGURE 6: Dependence of k' on CAP concentration with TPCK–trypsin. The values of k' were generated as described in the legend to Figure 2. The data points were fitted to eq 4, a hyperbolic relationship that describes the behavior of k' as a function of inhibitor concentration for a two-step binding mechanism described by scheme B (see Results).

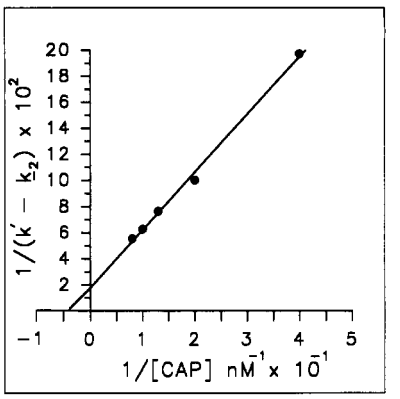

FIGURE 7: Dependence of $1/(k' - k_{-2})$ on $1/[CAP]$ concentration with TPCK–trypsin. The values of k' were generated as described in the legend to Figure 1. The value of k_{-2} was calculated to be 5.0 $\times$ 10^{-5} s^{-1} from the data shown in Figures 3 and 4 (see Results). The y-intercept is $1/k_2$, and the negative x-intercept is $-1/K_{i(app)}$, as previously described for a two-step binding mechanism (Shapiro & Riordan, 1984).

so that $k' \approx k_{-2}$. By this approach, k_{-2} was determined to be 5.0 $\times$ 10^{-5} s^{-1}, in close agreement with the value reported above.

Establishment of the values for k_{-2}, K_i, and K_i', enabled the forward isomerization rate constant, k_2, to be calculated from the rearranged definition of the overall inhibition constant:

$$k_2 = [(K_i/K_i')(k_{-2})] - k_{-2} \quad (3)$$

A value of 5.3 $\times$ 10^{-3} s^{-1} ($\pm$1.4 $\times$ 10^{-3}, SD, n = 4) was calculated for k_2 using eq 3. In addition, k_2 was also determined from plots of k' versus CAP concentration. In both mechanisms described by schemes A and B, k' increases with an increase in inhibitor concentration (Morrison & Walsh, 1988). In theory, plots of k' versus inhibitor concentration can be used to distinguish between these two mechanisms. In mechanism A, k' increases as a linear function of the inhibitor concentration, while in mechanism B, k' increases as a hyperbolic function of inhibitor concentration and reaches a lower and upper limit equal to k_{-2} and $(k_2 + k_{-2})$, respectively (Morrison & Walsh, 1988). The observed increase in k' over the range of CAP concentrations used in reactions with TPCK–trypsin could be fitted to the following hyperbolic equation that characterizes the two-step mechanism shown in scheme B (Morrison & Walsh, 1988):

$$k' = k_{-2} + k_2[([I]/K_i)/(1 + [S]/K_m + [I]/K_i)] \quad (4)$$

A value of k_2 was estimated to be 6.2 $\times$ 10^{-3} s^{-1} ($\pm$1.6 $\times$ 10^{-3}, SD, n = 4) from the best fit hyperbola through the data points in Figure 6. In practice, the use of eq 4 to further discriminate between mechanism A and mechanism B was inconclusive since linear regression also generated a good fit through the data points. Higher concentrations of CAP are unlikely to generate a more authentic hyperbola due to the sensitivity limitations inherent in the methodology employed. Therefore, to discriminate between a single-step and a two-step mechanism based on k', we utilized the graphical transformation previously reported by Shapiro and Riordan (1984). Double-reciprocal plots of $1/(k' - k_{-2})$ versus $1/[I]$ are linear for both mechanisms, but in mechanism A, the line passes through the origin, while in mechanism B the line passes through the y-intercept. Figure 7 is a double-reciprocal plot using the values of k' and k_{-2} previously determined for the interaction of CAP with TPCK–trypsin. The best fit line through the data points passed through the y-intercept, consistent with the two-step mechanism described by scheme B. These findings also justify the use of a hyperbola to estimate k_2 from the k' versus [CAP] plot in Figure 6. The y-intercept in Figure 7 is $1/k_2$, from which k_2 was calculated to be 5.7 $\times$ 10^{-3} s^{-1} ($\pm$1.0 $\times$ 10^{-3}, SD, n = 4), in reasonable agreement with the value of k_2 determined using eqs 3 and 4. The negative x-intercept in Figure 7 is $-1/K_{i(app)}$, from which K_i was estimated to be 1.5 nM, in agreement with the value calculated from V_{max}/v_0 versus [CAP] plots (Figure 3). The individual inhibition constants and rate constants for the two-step inhibition of TPCK–trypsin by CAP are summarized in Table 1.

In addition to trypsin, CAP also has been shown to inhibit the amidolytic activity of human factor Xa (Morgenstern et al., 1993). Figure 8 shows a family of reaction progress curves for the inhibition of factor Xa by various concentrations of CAP. As the concentration of CAP was increased, the initial burst phase of each curve remained virtually unchanged, while the transition to steady-state equilibrium occurred faster, with an increase in the inhibitor concentration. Fitting the data to the slow-binding equation (eq 1) revealed that the initial velocity was independent of CAP concentration. The overall first-order rate constant, k', was also found to increased with an increase in CAP concentration. Therefore, the interaction of CAP with factor Xa followed the simplest model for the formation of an inhibitory complex described by scheme A. In accordance with a single-step mechanism, eq 2 simplifies to the following relationship (Morrison & Walsh, 1988):

$$k' = k_{-1} + k_1([I]/(1 + [S]/K_m)) \quad (5)$$

Equation 5 predicts a linear fit through the data points of a k' versus inhibitor concentration plot. From the slope of the line k_1 was calculated to be 1.3 $\times$ 10^5 M^{-1} s^{-1} ($\pm$0.3 $\times$ 10^5, SD, n = 7) (Figure 9). The first-order dissociation rate constant, k_{-1}, was determined from the y-intercept to be 4.8 $\times$ 10^{-4} s^{-1} ($\pm$1.2 $\times$ 10^{-4}, SD, n = 7). Additional evidence for the single-step interaction of CAP with factor Xa was obtained from the findings that plots of $1/(k' - k_{-1})$ versus $1/[CAP]$ were linear and passed through the origin (Figure 10). The overall inhibition constant, K_i', for the single-step interaction of factor Xa with CAP was calculated to be 3.7 nM. The K_i' was determined from the k_{-1}/k_1 ratio using the values generated from the k' versus [CAP] plot shown in Figure 9. The rate constants and the overall inhibition constant for the interaction of CAP with factor Xa are summarized in Table 1.

Table 1: Kinetic Constants for the Interaction of CAP with TPCK–Trypsin and Factor Xa

proteinase	K_i (k_{-1}/k_1, nM)	K_i' (pM)	k_2 (10^{-3} s^{-1})	k_{-2} (10^{-5} s^{-1})	k_2/K_i (10^6 M^{-1} s^{-1})	k_{assoc} (10^6 M^{-1} s^{-1})
TPCK–trypsin[a]	2.0	22.5[c]	5.7[c]	5.0[c]	2.85	2.8[d]
proteinase		K_i' (k_{-1}/k_1, nM)		k_1 (10^5 M^{-1} s^{-1})		k_{-1} (10^{-4} s^{-1})
factor Xa[b]		3.7		1.3		4.8

[a] Inhibition of TPCK–trypsin by CAP followed a two-step mechanism. [b] Inhibition of factor Xa by CAP followed a single-step mechanism. [c] Numbers represent the mean of values determined by different methods. [d] Determined using the method described by Tain and Tsou (1982).

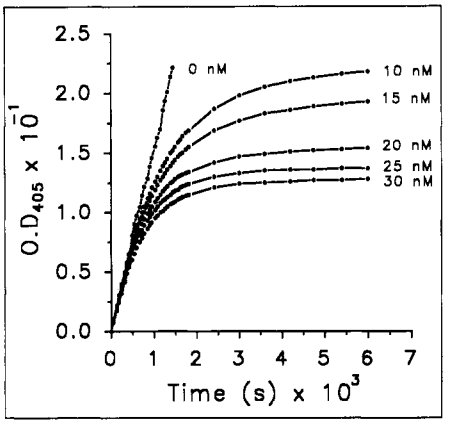

FIGURE 8: Slow-binding kinetics for the inhibition of human factor Xa by CAP. Factor Xa (0.3 nM) was reacted with 0, 10, 15, 20, 25, and 30 nM CAP in 20 mM Hepes (7.5)/0.15 M NaCl/0.01% BSA/0.5% glycerol/0.75 mM S-2222. The reactions were monitored continuously for 5 h at 405 nm, and the data were fitted to eq 1 to generate the variables v_0, v_s, and k' (Materials and Methods). To emphasize the similarity of the initial segment in each progress curve, only the initial 1.7 h of each reaction is presented.

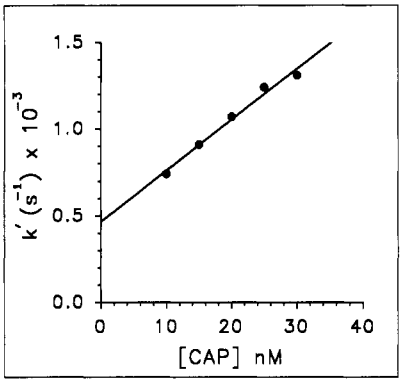

FIGURE 9: Dependence of k' on CAP concentration with human factor Xa. The values of k' were generated as described in the legend to Figure 8 and represent the mean values of $n = 7$ experiments. The data points were fitted to eq 5 in accordance with the single-step binding mechanism described by scheme A (see Results). The slope of the line is $k_1/(1 + [S]/K_m)$, and the intersecting point on the y-intercept is k_{-1}. The standard deviations for k_1 and k_{-1} are reported in Results.

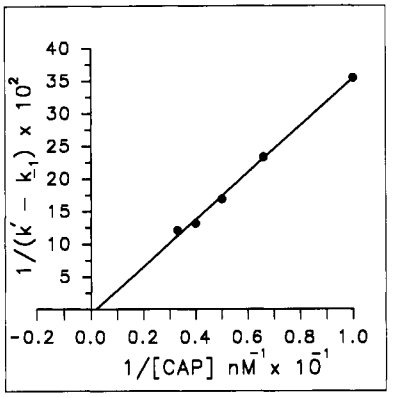

FIGURE 10: Dependence of $1/(k' - k_{-1})$ on $1/[CAP]$ concentration with human factor Xa. The values of k' were generated as described in the legend to Figure 9. The value of k_{-1} used was calculated to be 4.8×10^{-4} s^{-1} from the data shown in Figure 9. In accordance with the single-step binding mechanism described by scheme A (see Results), the best fit line passed through the origin (Shapiro & Riordan, 1984).

DISCUSSION

In the present study, we have deduced the primary structure and kinetic properties of a novel intracellular serine proteinase inhibitor. On the basis of several structural criteria (Remold-O'Donnell, 1993), the cytoplasmic antiproteinase represents a new member of the ovalbumin family of cytoplasmic serpins. A prominent feature that links CAP to this unique serpin branch is the absence of a cleavable N-terminal hydrophobic signal peptide, yet family members reside either intracellularly, extracellularly, or both. Ovalbumin is a glycoprotein that is secreted into the extracellular milieu. Several regions within the ovalbumin primary structure have been shown to function as an internal signal sequence (Lingappa et al., 1979; Tabe et al., 1984), and a significant amount of amino acid identity was found in the corresponding regions of CAP. A hydrophobic region (residues 218–235) in ovalbumin was previously shown to exhibit identity with the N-terminal cleavage signals of other secreted proteins (Lingappa et al., 1979). Unlike ovalbumin, this hydrophobic sequence in CAP was interrupted by Lys-226 and Glu-227, which may explain the observed retention of CAP in the cytoplasm of cells (Couglin et al., 1993; Eaton & Baker, 1983; Morgenstern et al., 1993). CAP was found to contain three potential N-glycosylation consensus sites. Under normal conditions, the cytoplasmic inhibitor does not appear to contain covalently attached sugar since CAP lacks an affinity for concanavalin A–Sepharose.[2]

The reactive-site domain of the serpins exhibits a high degree of divergence, which probably reflects an optimal conformation for a high-affinity association with the substrate binding cleft of their cognate proteinases (Bode & Huber, 1992). Inspection of the cytoplasmic antiproteinase reactive site suggests that CAP inhibitory capabilities may extend to a wide variety of proteinases. For example, a cysteine residue in the P_1' position is unique to the mammalian serpins and is found in a cytoplasmic serpin encoded by the *crmA* gene of the cowpox virus (Pickup et al., 1986). The viral serpin has been previously shown to inhibit the interleukin-1β converting enzyme, a novel cysteine proteinase (Ray et al., 1992). In addition, the presence of several methionine residues and a cysteine in the reactive-site region of CAP suggests that the inhibitory activity may be sensitive to oxidation. This possibility correlates with the intracellular localization of CAP and agrees with our finding that reducing agents, such as β-mercaptoethanol, appear to stabilize CAP activity during purification from both cultured cells (Morgenstern et al., 1993) and human placenta (Materials and Methods). Under certain circumstances, it is conceivable

[2] K. Morgenstern and W. Kisiel, unpublished results.

that Met-340 of CAP could function as the P_1 proteinase specificity residue and Arg-341 as a monobasic residue in the P_1' position. The presence of multiple cleavage sites in the reactive center of a serpin is not unprecedented and has been demonstrated for the inhibition of plasmin and chymotrypsin by α_2-antiplasmin (Potempa et al., 1988).

It has been previously proposed that the reactive-site domain serves as a pseudosubstrate for the proteinase (Beatty et al., 1980; Carrell & Boswell, 1986) and results in the formation of an initial complex comparable to a Michaelis complex in an enzyme–substrate reaction (Longstaff & Gaffney, 1991). However, unlike a typical substrate, the proteinase–serpin complex then undergoes a dramatic conformational change that appears to be essential for the mechanism of proteinase inactivation (Björk et al., 1992, 1993; Lodermann et al., 1984; Skriver et al., 1991). Therefore, serpins would appear to operate by a common pathway that involves two equilibria, the rapid binding of a loose P·I complex and a isomerization step to a tight, more stable, P·I complex. Olson and Shore (1982) detected a two-step mechanism for the inhibition of thrombin by antithrombin III using a *p*-aminobenzamidine displacement method with stopped-flow fluorimetry. Bruch and Bieth (1989) used a similar approach and report evidence for a two-step binding mechanism for the inhibition of chymotrypsin by α_1-proteinase inhibitor. Recently, with the application of the slow-binding kinetic approach (Morrison & Walsh, 1988), the inhibition of plasmin and chymotrypsin by α_1-antiplasmin (Longstaff & Gaffney, 1991) and the inhibition of neutrophil elastase by α_2-proteinase inhibitor (Faller et al., 1993) have been found to follow a two-step binding mechanism. However, within this mechanistic framework, these serpins appear to behave differently. The inhibition of thrombin by antithrombin III (Olson & Shore, 1982) and the inhibition of chymotrypsin (Bruch & Bieth, 1989) and neutrophil elastase (Faller et al., 1993) by α_1-proteinase inhibitor form very loose initial P·I complexes, with K_i values of 4 μM, 0.19 mM, and 80 nM, respectively. These complexes are then rapidly converted to a stable tight P·I complex. On the other hand, α_2-antiplasmin inhibition of plasmin and chymotrypsin forms a tight initial complex, with K_i values of 8 nM and 6.6 nM, respectively, which then slowly converts to the a more stable P·I complex (Longstaff & Gaffney, 1991). These findings have lead to the proposal that serpins use a variety of combinations of kinetic parameters to arrest the physiological mechanism of proteolysis (Faller et al., 1993).

We have characterized the inhibition kinetics of the cytoplasmic antiproteinase using trypsin and factor Xa as two highly divergent model proteinases. To our knowledge, this is the first investigation to detail the mechanism of proteinase inhibition by an intracellular serpin. The cytoplasmic antiproteinase was found to inhibit TPCK–trypsin by a two-step binding mechanism that involved the rapid preequilibrium of a loose complex, which was then converted slowly to a more stable, tight complex. Under the appropriate conditions, reversibility of the TPCK–trypsin·CAP tight complex could be observed. These results correlate with our initial findings that CAP forms a high-affinity reversible complex with anhydrotrypsin–agarose, suggesting that a covalent intermediate is not absolutely necessary for a stable proteinase·CAP interaction (Morgenstern et al., 1993). In addition, Kirshner and co-workers (Kirshner et al., 1980) demonstrated that the cytoplasmic inhibitor could be released from a trypsin–agarose affinity column when the column was incubated with an excess of lima bean trypsin inhibitor. However, previous studies have demonstrated that both crude (Coughlin et al., 1993; Eaton & Baker, 1983) and purified (Morgenstern et al., 1993) preparations of CAP form an SDS-stable complex with serine proteinases, suggesting that the proteinase·CAP complex may be stabilized in a reversible tetrahedral intermediate that is induced to collapse to an acyl linkage by denaturants. A tetrahedral intermediate was previously detected in the complex between neutrophil elastase and α_1-proteinase inhibitor (Matheson et al., 1991). The overall binding equilibrium between TPCK–trypsin and CAP was measured to be 22.5 pM, demonstrating that CAP is a very potent inhibitor of this proteinase. The initial loose complex formed with a dissociation constant of approximately 2 nM. Therefore, we conclude that the reaction between TPCK–trypsin and CAP behaves similarly to the previously described inhibition of chymotrypsin and plasmin by α_2-antiplasmin (Longstaff & Gaffney, 1991). The formation of the initial complex between TPCK–trypsin and CAP was approximately 3- to 4-fold tighter than reported for α_2-antiplasmin inhibition of chymotrypsin and plasmin, respectively. However, the TPCK–trypsin·CAP loose complex is converted to the tight complex at a rate (5.7×10^{-3} s^{-1}) which is very comparable to the forward isomerization rate previously reported for chymotrypsin·α_2-antiplasmin (9×10^{-3} s^{-1}) and plasmin·α_2-antiplasmin (6×10^{-3} s^{-1}) complexes (Longstaff & Gaffney, 1991). The primary difference between the measured rate constants for the inhibition of TPCK–trypsin by CAP and the inhibition of plasmin by α_2-antiplasmin was the reverse isomerization step. Therefore, our TPCK–trypsin inhibition studies are entirely consistent with the results of Longstaff and Gaffney (1991) and substantiate the hypothesis that k_{-2} is an important criterion for the overall binding strength of some proteinase·serpin interactions. In all likelihood, the magnitude of k_{-2} reflects the degree of strain released from the native serpin reactive-site loop during formation of the tight complex and the stability of the resulting tetrahedral intermediate.

In addition to TPCK–trypsin, we have characterized the kinetics between factor Xa and the cytoplasmic antiproteinase. In contrast to the reaction between TPCK–trypsin and CAP, CAP inhibited the amidolytic activity of factor Xa by a single-step binding mechanism. The overall inhibition constant for this single-step inhibition reaction was approximately 4 nM with a second-order association rate constant of 1.3×10^5 M^{-1} s^{-1}. The inability to detect a loose complex in the reaction pathway for factor Xa inhibition by CAP may be due to the fact that $K_i \gg K_i'$, in the putative two-step mechanism (Morrison & Walsh, 1988). In this case, slow binding may be observed because CAP initially encounters significant energy barriers for the correct alignment with the substrate binding cleft of factor Xa. However, once aligned, the factor Xa·CAP interaction is strong and results in a slower rate of dissociation. Although this possibility cannot be readily distinguished from a strict single-step binding mechanism, an initial transient interaction has been described for other slow-binding inhibitors (Stone et al., 1984) and is entirely consistent with the restricted substrate specificity known to be a physiological feature of factor Xa activity.

REFERENCES

Astrup, T. (1978) *Prog. Chem. Fibrinolysis Thrombolysis 3*, 1–57.

Beatty, K., Bieth, J., & Travis, J. (1980) *J. Biol. Chem. 255*, 3931–3934.

Björk, I., Nordling, K., Larsson, I., & Olson, S. T. (1992) *J. Biol. Chem. 267*, 19047–19050.
Björk, I., Nordling, K., & Olson, S. T. (1993) *Biochemistry 32*, 6501–6505.
Bode, W., & Huber, R. (1992) *Eur. J. Biochem. 204*, 433–451.
Bruch, M., & Bieth, J. G. (1989) *Biochem. J. 259*, 929–930.
Carrell, R. W., & Boswell, D. R. (1986) in *Proteinase Inhibitors* (Barrett, A., & Salvesen, G., Eds.) pp 403–420, Elsevier, New York.
Carrell, R. W., Pemberton, P. A., & Boswell, D. R. (1987) *Cold Spring Harbor Symp. Quant. Biol. 52*, 527–535.
Cha, S. (1975) *Biochem. Pharmacol. 24*, 2177–2185.
Chase, T., & Shaw, E. (1969) *Biochemistry 8*, 2212–2224.
Coughlin, P. B., Tetaz, T., & Salem, H. H. (1993) *J. Biol. Chem. 268*, 9541–9547.
Davie, E. W., Fujikawa, K., & Kisiel, W. (1991) *Biochemistry 30*, 10363–10370.
Doolittle, R. F. (1983) *Science 222*, 417–419.
Dubin, A., Travis, J., Enghild, J. J., & Potempa, J. (1992) *J. Biol. Chem. 267*, 6576–6583.
Eaton, D. L., & Baker, J. B. (1983) *J. Cell. Physiol. 117*, 175–182.
Faller, B., Cadène, M., & Bieth, J. G. (1993) *Biochemistry 32*, 9230–9235.
Flint, I. L., Bailey, T. J., Gustafson, T. A., Maekham, B. E., & Morkin, E. (1986) *Proc. Natl. Acad. Sci. U.S.A. 83*, 7708–7712.
Huber, R., & Carrell, R. W. (1989) *Biochemistry 28*, 8951–8966.
Hunt, L. T., & Dayhoff, M. O. (1980) *Biochem. Biophys. Res. Commun. 95*, 864–871.
Joslin, G., Wittwer, A., Adams, S., Tollefsen, D. M., August, A., & Perlmutter, D. H. (1993) *J. Biol. Chem. 268*, 1886–1893.
Kirschner, R. J., Federiuk, C. S., Ford, J. P., & Shafer, J. A. (1980) *J. Biol. Chem. 255*, 5468–5474.
Kisiel, W., & Davie, E. W. (1975) *Biochemistry 14*, 4928–4934.
Kondo, S., & Kisiel, W. (1987) *Blood 70*, 1947–1954.
Kozak, M. (1986) *Cell 44*, 283–292.
Leatherbarrow, R. J. (1987) *Enzfitter, a program for nonlinear regression analysis*, Elsevier Scientific, New York.
Lingappa, V. R., Lingappa, J. R., & Blobel, G. (1979) *Nature 281*, 117–121.
Lodermann, H., Tokuoka, R., Deisenhofer, J., & Boswell, D. R. (1984) *J. Mol. Biol. 177*, 531–556.
Longstaff, C., & Gaffney, P. J. (1991) *Biochemistry 30*, 979–986.
Mahoney, W. C., Kurachi, K., & Hermodson, M. A. (1980) *Eur. J. Biochem. 105*, 545–552.
Maniatis, T., Fritsch, E. F., & Sambrook, J. (1989) *Molecular Cloning: A Laboratory Manual*, 2nd ed., Cold Spring Harbor Laboratory, Cold Spring Harbor, NY.
Mast, A. E., Enghild, J. J., Pizzo, S. V., & Salvesen, G. (1991) *Biochemistry 30*, 1723–1730.
Matheson, N. R., Halbeek, H. V., & Travis, J. (1991) *J. Biol. Chem. 266*, 13489–13491.
Moore, C. L., & Sharp, P. A. (1985) *Cell 41*, 845–855.
Morgenstern, K. A., Henzel, W. J., Baker, J. B., Wong, S., & Kisiel, W. (1993) *J. Biol. Chem. 268*, 21560–21568.
Morrison, J. F. (1982) *Trends Biochem. Sci. 7*, 102–105.
Morrison, J. F., & Walsh, C. T. (1988) *Adv. Enzymol. 61*, 201–301.
Neurath, H. (1984) *Science 224*, 340–357.
Olson, S. T., & Shore, J. D. (1982) *J. Biol. Chem. 257*, 14891–14895.
Pickup, D. J., Ink, B. S., Hu, W., & Joklik, W. K. (1986) *Proc. Natl. Acad. Sci. U.S.A. 83*, 7698–7702.
Potempa, J., Shieh, B.-H., & Travis, J. (1988) *Science 241*, 699–700.
Ray, C. A., Black, R. A., Kronheim, S. R., Greenstreet, T. A., Sleath, P. R., Salvesen, G. S., & Pickup, D. J. (1992) *Cell 69*, 597–604.
Reid, K. B., & Porter, R. R. (1981) *Annu. Rev. Biochem. 50*, 443–464.
Remold-O'Donnell, E. (1993) *FEBS Lett. 315*, 105–108.
Remold-O'Donnell, E., Chin, J., & Alberts, M. (1992) *Proc. Natl. Acad. Sci. U.S.A. 89*, 5635–5639.
Saksela, O., & Rifkin, D. B. (1988) *Annu. Rev. Cell Biol. 4*, 93–126.
Sanger, F., Nicklen, S., & Coulson, A. R. (1977) *Proc. Natl. Acad. Sci. U.S.A. 74*, 5463–5467.
Schechter, I., & Berger, A. (1967) *Biochem. Biophys. Res. Commun. 27*, 157–162.
Shapiro, R., & Riordan, J. F. (1984) *Biochemistry 23*, 5234–5240.
Skiver, K., Wikoff, W. R., Patston, P. A., Tausk, F., Schapira, M., Kaplan, A. P., & Bock, S. C. (1991) *J. Biol. Chem. 266*, 9216–9221.
Stone, S. R., Montgomery, J. A., & Morrison, J. F. (1984) *Biochem. Pharmacol. 33*, 175–179.
Suminami, Y., Kishi, F., Sekiguchi, K., & Kato, H. (1991) *Biochem. Biophys. Res. Commun. 181*, 51–58.
Tabe, L., Krieg, P., Strachan, R., Jackson, D., Wallis, E., & Colman, A. (1984) *J. Mol. Biol. 180*, 645–666.
Tian, W.-X., & Tsou, C.-L. (1982) *Biochemistry 21*, 1028–1032.
Travis, J., Bowen, J., Tewksbury, D., Johnson, D., & Pannell, R. (1976) *Biochem. J. 157*, 301–306.
Ye, R. D., Ahern, S. M., Le Breau, M. M., Lebo, R. V., & Sadler, L. E. (1989) *J. Biol. Chem. 264*, 5495–5502.